OXFORD

SOT | Society of Toxicology
www.toxsci.oxfordjournals.org

TOXICOLOGICAL SCIENCES, 167(2), 2019, 385–396

doi: 10.1093/toxsci/kfy244
Advance Access Publication Date: September 22, 2018
Research Article

Trovafloxacin-Induced Liver Injury: Lack in Regulation of Inflammation by Inhibition of Nucleotide Release and Neutrophil Movement

Giulio Giustarini,* Nienke Vrisekoop,† Laura Kruijssen,* Laura Wagenaar,* Selma van Staveren,† Manon van Roest,* Rob Bleumink,* Marianne Bol-Schoenmakers,* Richard J. Weaver,‡ Leo Koenderman,† Joost Smit,* and Raymond Pieters*,[1]

*Immunotoxicology, Faculty of Veterinary Medicine, Institute for Risk Assessment Sciences, Yalelaan 104, 3584CM, Utrecht University, Utrecht, The Netherlands; †Department of Respiratory Medicine and Laboratory of Translational Immunology (LTI), University Medical Center Utrecht, Heidelberglaan 100, 3584CX, Utrecht, The Netherlands; and ‡Institut de Recherches Internationales Servier (I.R.I.S.), Suresnes 92284, France

[1]To whom correspondence should be addressed at Dr. Raymond Pieters, Yalelaan 104, 3584CM Utrecht, The Netherlands. E-mail: r.h.h.pieters@uu.nl.

ABSTRACT

The fluoroquinolone trovafloxacin (TVX) is associated with a high risk of drug-induced liver injury (DILI). Although part of the liver damage by TVX+TNF relies on neutrophils, we have recently demonstrated that liver recruitment of monocytes and neutrophils is delayed by TVX. Here we show that the delayed leukocyte recruitment is caused by a combination of effects which are linked to the capacity of TVX to block the hemichannel pannexin 1. TVX inhibited find-me signal release in apoptotic HepG2 hepatocytes, decelerated freshly isolated human neutrophils toward IL-8 and f-MLF, and decreased the liver expression of ICAM-1. In blood of TVX+TNF-treated mice, we observed an accumulation of activated neutrophils despite an increased MIP-2 release by the liver. Depletion of monocytes and neutrophils caused increased serum concentrations of TNF, IL-6, and MIP-2 in TVX-treated mice as well as in mice treated with the fluoroquinolone levofloxacin, known to have a lower DILI-inducing profile. This supports the idea that early leukocyte recruitment regulates inflammation. In conclusion, disrupted regulation by leukocytes appears to constitute a fundamental step in the onset of TVX-induced liver injury, acting in concert with the capability of TVX to induce hepatocyte cell death. Interference of leukocyte-mediated regulation of inflammation represents a novel mechanism to explain the onset of DILI.

Key words: DILI; trovafloxacin; neutrophils; monocytes; regulation of inflammation; nucleotide release.

Immune-mediated drug-induced liver injury (i-DILI) is a drug-specific adverse response determined by individual factors, both inherent and environmental. i-DILI is an important socio-economic problem, particularly because it is difficult to predict it preclinically and it becomes apparent in human clinical trials or in clinical practice.

Anti-microbials are an important group of pharmaceuticals linked to i-DILI as they represent almost half of the total number of observed cases (Chalasani *et al.*, 2015). Combined with the urgent need for new safe therapies to counteract resistant microbes, mechanistic knowledge on how anti-microbials cause i-DILI is highly warranted.

The fluoroquinolone antibiotic trovafloxacin (TVX) was withdrawn from the market in 2001 due to a high incidence of DILI, only 3 years after its market introduction. Animal studies investigating the mechanism of toxicity mediated by TVX (Shaw *et al.*, 2007, 2009c) revealed the importance of co-exposure to microbial substances, such as lipopolysaccharide

(LPS), as key factor in the development of TVX-induced liver injury. Subsequent studies identified the pro-inflammatory cytokine TNF as a proximal common mediator in the pathogenesis of TVX-induced i-DILI (Shaw *et al.*, 2009d). Also other pharmaceuticals associated with DILI in patients have been demonstrated to cause liver damage in rodents when combined with LPS or TNF (Deng *et al.*, 2006; Gandhi *et al.*, 2013; Lu *et al.*, 2013; Luyendyk *et al.*, 2003).

Studies showing that TVX-induced liver damage is reduced in mice deficient in neutrophil elastase (Shaw *et al.*, 2009c) indicate that activation of neutrophils is crucial in TVX-induced DILI. However, recently we have shown that, although leukocytes are abundantly present when liver damage is apparent, TVX appears to cause a delay of TNF-elicited liver sequestration of neutrophils and monocytes (Giustarini *et al.*, 2018). This finding is of particular significance in view of the recently acknowledged role of these cells in the resolution of inflammation (Soehnlein and Lindbom, 2010).

Importantly, it has also been demonstrated that TVX, at concentrations relevant to those found in the serum of human treated with TVX (≈ 5 μM) (Vincent *et al.*, 1998), blocks the hemichannel pannexin 1 (PNX1) (Poon *et al.*, 2014). Further studies evaluating the role of immune cells in infection and inflammation identified PNX1 as a key player in the regulation of pathophysiological processes especially involving phagocytes (Lohman *et al.*, 2015). When activated, PNX1 releases small molecules (such as ATP and UTP) capable of stimulating innate cell functions in autocrine and paracrine fashions. These small molecules are considered "find-me" signals attracting immune cells toward dying cells, but are also found to be crucial for the actual migration of leukocytes. In addition, PNX1 blockade has been shown to reduce the expression of vascular cell adhesion molecule 1, the vascular adhesion molecule for leukocytes (Lohman *et al.*, 2015).

Therefore, we hypothesized that PNX1-dependent exacerbation of inflammatory responses represents a key event in TVX-mediated i-DILI. We investigated whether TVX influences key processes that can be linked to PNX1 interference, eg, release of find-me signals, neutrophil migration, and ICAM-1 expression. Our data shows that TVX, but not its non-iDILI-associated structural homologue levofloxacin (LVX), blocks the PNX1-hemichannel on dying hepatocytes. In addition, data shows that TVX decelerates human neutrophil movements and decreases ICAM-1 expression in vivo. The TVX-induced PNX1 blockade may thus result in a combination of cellular events that provide a novel explanation for the idiosyncrasy of TVX-induced DILI. The idiosyncratic nature of DILI may reside in a kinetics of innate immune responses that may vary per individual. In certain individuals the combination of TVX administration with fluctuant and circadian cytokine concentrations during antimicrobial activity of innate immune responses may increase pro-inflammatory responses due to the suppression of an appropriate regulatory cellular response.

MATERIALS AND METHODS

Animals

Male, 9 to 11-week old, C57BL/6J mice (The Jackson Laboratory, Charles River) were used for all experiments. They were allowed to acclimatize for 1 week in a 12-h light/dark cycle and maintained at mean temperature of 23 ± 2°C, 50–55% relative humidity. Acidified drinking water and laboratory food pellets were provided ad libitum.

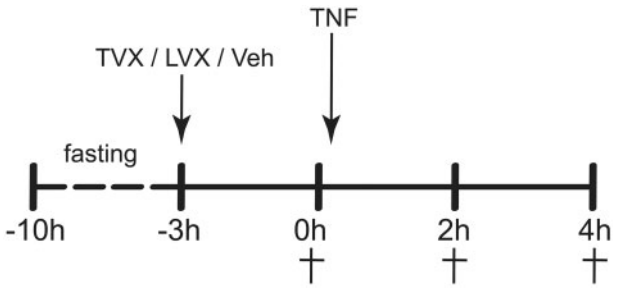

Figure 1. Protocol for the treatment of mice in the TVX+TNF model of DILI. Mice were fasted for 7 h and then administered with an intragastric gavage of the drug solution or vehicle. Three hours later, mice were either sacrificed to observe the effects of the drugs or intraperitoneal injection of TNF was performed. TNF-injected mice were subsequently sacrificed at 2 and 4 h after the injection with the cytokine.

In vivo studies were approved by the Ethics Committee for Animal Experiments of Utrecht University and complied with governmental and international guidelines on animal experimentation (CCD permission number: AVD108002016503).

Human blood cells

Ethical approval for obtaining healthy human volunteer blood was obtained by the institutional ethical review board of the University Medical Centre Utrecht (UMCU) and all subjects provided written informed consent.

Compounds and chemicals

Trovafloxacin (TVX), levofloxacin (LVX), and N-formyl-methionyl-leucyl-phenylalanine (f-MLF) were purchased from Sigma-Aldrich (St. Louis, Missouri). Recombinant murine TNF was purchased from R&D Systems (Minneapolis, Minnesota). IL-8 (72 aa) was obtained from PeproTech (Rocky Hill, New Jersey).

In vivo experimental set up and depletion of Ly6C+ cells

Mice were fasted 7 h prior to treatment. TVX (150 mg/kg), LVX (375 mg/kg), or saline vehicle (Veh) was administered orally 3 h before recombinant murine TNF injection (50 μg/kg, i.p.) (Shaw *et al.*, 2009b). Food was available again immediately after TNF administration. Animals analyzed at time point 0 h did not receive TNF (Figure 1). Concentration of TVX was determined by a previous study showing that 150 mg/kg TVX interacts with LPS-induced TNF to increase serum ALT and induce histopathological liver modifications which were not observed with the administration of the drug only (Shaw *et al.* 2007).

To deplete neutrophils and monocytes/macrophages, mice were treated with anti-Ly6C (200 μg/mouse, i.p., 250 μl) or with the corresponding isotype (IgG2b, 200 μg/mouse, i.p., 250 μl) 72 and 24 h before receiving the drug solutions.

Mouse blood, spleen, and intra-hepatic leukocyte isolation

Blood from inferior vena cava was collected in pre-coated lithium heparin tubes and centrifuged for 6 min at 2000 rpm. Intrahepatic leukocytes were isolated as described previously by Crispe *et al.* (Crispe, 2001). Briefly, liver was perfused with 5 ml ice-cold PBS and excised from the animal. Tissue was minced and gently passed through a sieve. The liver slurries were centrifuged, and the pellet resuspended with a collagenase D (0.02%, w/v) and DNAse I (0.002%, w/v) solution.

The suspensions were incubated at 37°C for 40 min on a reciprocating shaker. Liver leukocytes were isolated by using a 45–67.5% isotonic Percoll density gradient (GE Healthcare, Fisher Scientific, Landsmeer, The Netherlands). Hepatic leukocytes obtained from Veh-only-treated mice (w/o TNF) were used as an internal control. With this we ruled out small day-by-day differences in the isolation efficiency throughout the experiments.

Leukocytes from mouse spleen were obtained forcing the organ to pass through a 70-μm strainer, after which single cells were washed once. To remove erythrocytes, cells were incubated with hypotonic red blood cell lysis buffer (containing NH_4Cl, $KHCO_3$, and Na_2EDTA) for 1 min, and washed once with PBS.

Human neutrophil isolation and 3D chemotaxis migration assay

Neutrophils were isolated as described previously from fresh whole blood by Overbeek *et al.* (2013). Neutrophil preparations consisted of 95–97% neutrophils as determined by microscopic analysis of cytospin preparations. Neutrophils were resuspended in incubation buffer (20 mM Hepes, 132 mM NaCl, 6 mM KCl, 1 mM $MgSO_4$, 1.2 mM KH_2PO_4, supplemented with 1.0 mM $CaCl_2$, 5 mM glucose, 0.5% [w/v] HSA) and mixed with fibrinogen (2 mg/ml) and thrombin (2 Units/ml). The final concentration of the cell suspension was $3 \times 10_6$ cells/ml. For chemotaxis analysis IBIDI 3D chemotaxis slides were used (μ-Slide Chemotaxis 3D, ibidiTreat; Integrated BioDiagnostics [IBIDI], Munich, Germany). Cells in fibrin gel mixtures were pipetted in the central channels of the IBIDI 3D slide. The front chambers were filled with f-MLF (10^{-7} M) or IL-8 (50 ng/ml), whereas the other chamber with negative control incubation buffer. Concentrations of TVX or LVX were tested in combination with both chemoattractants. The slides were then transferred to an incubator hood (37°C) on a Leica DXMRE microscope and temperature equilibrated for at least 10 min, before multi-spot time-lapse imaging at 37°C was performed. Multi-spot time-lapse imaging was performed with a computer-assisted microscopy system (Quantimet for Windows, Qwin), DXMRE microscope, PL fluorostar low power objective lens to a magnification of 5× (Leica, Heidelberg, Germany). Sequences consisted of 100 images per spot with a maximum of 6 revisited spots. The time-lapse intervals were typically 15–25 s. Images were imported into the Optimas image analysis package (Media Cybernetics, Inc. Bethesda, Rockville, Maryland). Custom-made macros (Arithmetic Language for Images, ALI) were used to plot the migrating cells using threshold-based detection and nearest neighbor tracking. Tracks and final vectors of migrating cells were plotted and analyzed for speed, directness, and directionality. Each analysis incorporated several tens to hundreds of tracked cells. Values were normalized for the average migration distance and speed of neutrophils that were not stimulated with chemoattractants.

Cell culture of HepG2 cells

HepG2 human hepatoblastoma cells (American Type Culture Collection, Manassas, Virginia) were used. Cells were maintained in MEM+Glutamax (Gibco, Invitrogen, Carlsbad, California) supplemented with 10% fetal bovine serum in 75 cm^2 tissue culture-treated flasks. Cells were cultured in a humidified atmosphere composed of 95% air and 5% CO_2 and a temperature of 37°C. Cells were passaged twice each week. About 0.25% Trypsin-EDTA was used to detach confluent HepG2 cells from the flask. After plating, cells were allowed 48 h to adhere before treatment. TVX and LVX was reconstituted to a stock solution of 200 mM in dimethyl sulfoxide (DMSO) and diluted in culture medium to the desired concentrations. The final DMSO concentrations did not exceed 0.1%. TNF was reconstituted to a stock solution of 100 μg/ml in PBS+BSA 0.1% as indicated by the manufacturer. After incubation with the fluoroquinolones with or without TNF, HepG2 cells were treated with Trypsin for 5 min before to add complete medium, and after prepared for flow cytometric analysis.

Flow cytometric analyses of liver and blood leukocytes and HepG2 cells

For flow cytometric analysis, cells were first stained with LIVE/DEAD® Fixable Dead Cell Stain (Molecular Probes, Invitrogen, Carlsbad, California) followed by incubation with anti-CD16/CD32 (clone 2.4G2) to block the FcR, stained with fluorescently labeled antibodies and stored in 1% paraformaldehyde until analysis. The following antibodies were used: anti-CD45.2 Pacific Blue (clone 104, Biolegend, Uithoorn, The Netherlands), anti-LY6G APC (clone 1A8, Biolegend), anti-F4/80 FITC (clone BM8, eBioscience, Halle-Zoersel, Belgium), anti-CD11b PE and FITC (clone M1/70, eBioscience), anti-Gr1 APC (clone RBG8C5, eBioscience) in fluorescence-activated cell sorting buffer (PBS containing 0.25% BSA, 0.05% NaN_3, 0.5 mM EDTA) for 30 min at 4°C.

HepG2 cells were stained with Annexin V-FITC, 7-AAD, and TO-PRO3 in Annexin V-binding buffer for 10 min at room temperature and immediately placed on ice until flow cytometric analysis.

Data were acquired by means of FACS Canto II and analyzed using Weasel flow analysis package (The Walter and Eliza Hall Institute of Medical Research, Melbourne, Australia).

Western blot analyses for ICAM-1

Approximately 50 mg of each mouse liver sample was lysed using 500 μL RIPA lysis buffer (Thermo-Fisher scientific, Rockford, Illinois) containing protease inhibitors (Roche Applied Science, Penzberg, Germany) and the total protein concentration was measured by the BCA protein assay kit (Thermo-Fisher scientific, Rockford, Illinois). Standardized protein amounts of boiled samples were isolated by electrophoresis in SDS-PAGE gel 4–10% and electro-transferred onto polyvinylidene difluoride membranes (Bio-Rad, Veenendaal, The Netherlands). Membranes were blocked with immersion in ethanol 100% for 1 min and after rehydrated with TBS supplemented with 0.2% Tween (TBS-T) and incubated overnight with polyclonal goat anti-mouse intercellular cellular adhesion molecule 1 (ICAM-1) antibody (1:1000, R&D Systems, Minneapolis, Minnesota). After washing in TBS-T, the membranes were incubated with rabbit anti-goat peroxidase-conjugated secondary antibody (1:5000, Dako, Glostrup, Denmark) for 1 h at room temperature. Finally, blots were washed in TBS-T and once in TBS, incubated with ECL Prime Western Blotting Detection Reagent (Amersham Biosciences, Roosendaal, The Netherlands), and digital images were obtained with the ChemiDoc XRS Quantity One (Bio-Rad Laboratories, Hercules, California). In the next step, the membranes were re-probed with a β-actin antibody (1:4000, Cell Signaling, Massachusetts) to assess the equality of loading. Signal intensities were quantified using ChemiDoc XRS Quantity One (Bio-Rad Laboratories, Hercules, California), and ICAM-1 expression normalized with β-actin and expressed as

the mean fold change in relation to samples obtained from mice receiving only the vehicle.

ELISA for MIP-2, IL6, and TNF

Blood from inferior vena cava was collected in pre-coated lithium heparin tubes. Plasma was used to determine ALT activity following the procedure reported in the manufacturer instruction (art. nr MAK052, Sigma-Aldrich, St. Louis, Missouri). TNF and IL-6 were determined in serum samples by sandwich ELISA. Antibodies were from eBioscience and procedures reported in the manufacturer instruction were followed. MIP-2 protein levels were evaluated in serum and liver tissue lysates obtained as described previously (Matzer *et al.*, 2001). For tissue lysates, total protein concentration was measured with BCA protein assay kit (Thermo-Fisher scientific, Rockford, Illinois). Analysis was performed according to manufacturer's protocol (Koma Biotech, Mouse MIP-2 ELISA core kit).

qPCR

For mRNA studies, the medial part of the biggest liver lobe from each mouse (approximately 50 mg) was snap frozen in liquid nitrogen and stored at −80°C until RNA isolation. Each sample was suspended in 500 µl RNA InstaPure (Eurogentec) and homogenized using a TissueLyser (Qiagen, Hilden, Germany) for 1 min/25 Hz twice. The homogenized tissue was centrifuged for 10 min at 12 000 × g. The supernatant containing RNA in RNA Insta-Pure was transferred to a new vial and RNA was isolated using phenol-chloroform extraction. The amount of RNA was determined using the NanoDrop 2000 Spectrophotometer (ThermoScientific). Subsequently, 1 µg of extracted total RNA was reverse transcribed with the iScriptTM cDNA Synthesis kit (Bio-Rad Laboratories, Hercules, California). Quantitative reverse transcriptase PCR was performed suing a iCycler iQ system (Biorad), and amplification was done using iQ SYBR Green supermix (Biorad) with 0.3 µM final primer concentration. Primer sequences: mouse MIP-2 FW-AAAGTTTGCCT TGACCCTGAAG and RV-CAGTTAGCCTTGCCTTTGTTCAGT.

Gene-specific primers for murine MIP-2 were derived from the NCBI GenBank and were manufactured commercially (Eurogentec, Seraing, Belgium). For each sample, mRNA expression was normalized for the detected Ct value of β-actin. Data are expressed as fold increase compared with the control group (vehicle only).

Statistical analyses

Data are presented as means ± standard error of the mean (SEM). Statistical significance for comparisons was determined by one- or two-way ANOVA with Dunnett's post hoc test. A *p*-value less than .05 was considered statistically significant. All data are analyzed using GraphPad Prism (version 6.07) software (San Diego, California).

RESULTS

TVX Decreases "Find Me" Signal Release From HepG2 Apoptotic Cells

Recently, Poon *et al.* (2014) have demonstrated that TVX prevents the release of damage-associated molecular patterns such as ATP, through blockade of PNX1 on early apoptotic cells. Since this action of TVX may be crucial to DILI, we first evaluated the opening of the PNX1 hemichannel on hepatocytes undergoing apoptosis induced by TVX+TNF.

To this end, HepG2 cells were exposed to TVX, LVX (concentration ranges 20–80 µM), or vehicle (Veh) only in presence or absence of TNF for 24 h. Cells were stained with 7-AAD and Annexin V-FITC in order to discriminate viable cells ($AnnV^-$/$7\text{-}AAD^-$), early apoptotic cells with unaffected membrane integrity ($AnnV^+$/$7\text{-}AAD^-$/$TO\text{-}PRO3^+$), permeabilized late apoptotic cells ($AnnV^+$/$7\text{-}AAD^+$/$TO\text{-}PRO3^+$), and apoptotic bodies ($AnnV^+$/$7\text{-}AAD^-$/$TO\text{-}PRO3^+$/FSC^{lo}) (Figure 2A). The fluorescent dye TO-PRO3 was used to determine the opening of the PNX1 channel since cells are impermeable to TO-PRO3 when PNX1 channel is closed. We thus evaluated the uptake of TO-PRO3 by flow cytometer following the gating strategy displayed in Figure 2A.

Co-incubation with TVX and TNF, but not with LVX or Veh and TNF, was associated with an increased amount of early and late apoptotic cells. TVX+TNF dose-dependently increased the number of early apoptotic cells when compared with the other treatments (Figure 2B, left panel). In these early apoptotic cells, phenotypically characterized as $AnnV^+$/$7\text{-}AAD^-$/$TO\text{-}PRO3^+$ cells, the median fluorescence intensity (MFI) for TO-PRO3 was decreased dose-dependently by TVX, indicating that TVX indeed blocks the PNX1 hemi channel (Figure 2B, right panel).

TVX Reduces Human Neutrophil Migration Toward Chemo-Attractants In Vitro

Because the hemichannel PNX1 (and ATP release) is known to be involved in neutrophil movement (Bao *et al.*, 2013; Kukulski *et al.*, 2009), we investigated the effect of TVX on the neutrophil chemotaxis toward gradients of two different chemoattractants: N-formyl-met-leu-phe (f-MLF) and IL-8.

Incubation of human neutrophils with increasing concentrations of TVX (range 1–10 µM) led to a dose-dependent decrease in neutrophil migration toward f-MLF or IL-8 (Figs. 3A and B, respectively). Incubation with TVX at 5 µM, the Cmax of the fluoroquinolone in human patients after oral therapy (Vincent *et al.*, 1998), resulted in ∼50% inhibition of neutrophil vector speed toward both chemoattractants.

No effects on chemotaxis to any of the two chemoattractants were observed when cells were incubated with 35 µM LVX (Figure 3). To exclude TVX cytotoxicity as a cause for decreased motility, TVX-treated neutrophils were tested for Annexin V and PI staining 4 h after incubation, and no significant differences in the percentage of viable cells were found with increased concentration of the drug up to 100 µM (Figure 3C).

TVX Increases MIP-2 in Liver and Serum and Reduces Hepatic ICAM-1 Expression

We also investigated the potential indirect (ie, not direct on neutrophils) mechanisms by which TVX may delay the influx of neutrophils in liver. For this reason, we quantified the amount of the main chemokine for neutrophils MIP-2 and the expression of ICAM-1, which is involved in their trapping in the liver at post-capillary venule level.

In line with the knowledge that PNX1 blockade reduces expression of adhesion molecules (Lohman *et al.*, 2015) TVX lowered the protein expression of ICAM-1, the receptor of CD11b/CD18, in liver tissue homogenates at 2 h (Figure 4A) and 4 h (data not shown) after exposure to TNF. LVX treatment led to mildly increased levels of ICAM-1 protein in TNF-treated mice (Figure 4A).

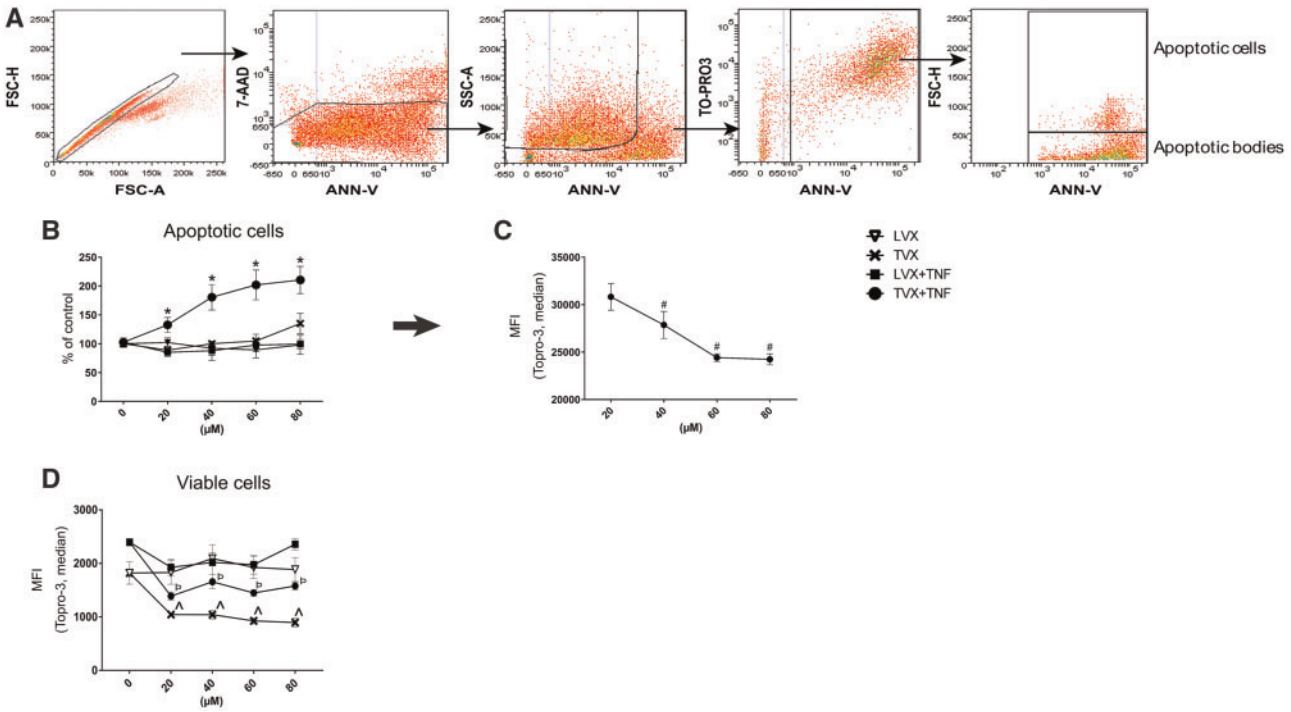

Figure 2. Increased concentration of TVX lowered TO-PRO3 staining in TVX+TNF-induced HepG2 apoptotic cells. HepG2 cells were incubated for 24 h with TVX, LVX, or vehicle with or without TNF. A, Gating strategy of apoptotic cells and bodies. B, Number of apoptotic cells are presented as percentage of cells counted in samples derived from HepG2 exposed only to vehicle (no TNF). C, TO-PRO3 median intensity in TVX+TNF-induced apoptotic cells. ● = TVX+TNF, ■ = LVX+TNF, × = TVX, ▼ = LVX. D, TO-PRO3 median intensity in viable cells. Data are presented as mean ± SEM; * $p < .05$ when compared with all the other treatments assessed, # $p < .05$ when compared with the lower dose of TVX causing increased amount of apoptotic cells (20 μM); Þ $p < .05$ when compared with cells exposed to DMSO (indicated as 0 for TVX and LVX),^ $p < .05$ when compared with cells exposed to DMSO+TNF (indicated as 0 for TVX+TNF and LVX+TNF), one-way ANOVA followed by Dunnett's post hoc test.

In contrast, the combination of TVX+TNF increased the serum MIP-2 concentrations (the murine functional analogue of the chemokine IL-8) when compared with the other treatments. TNF by itself already increased the serum levels of this cytokine in TVX-, LVX-, and vehicle-treated animals (Figure 4B), but pretreatment with TVX induced a significant increase of this cytokine compared with the other treatments at both 2 and 4 h after TNF administration. Notably, MIP-2 transcripts and protein levels were already increased in liver homogenates of TVX only-treated mice, so before exposure to TNF (Figure 4C).

TVX Induces Early Neutrophil Activation in Blood

As observed in our previous study (Giustarini *et al.*, 2018), the number of hepatic neutrophils were decreased early after TNF injection in TVX-treated mice when compared with none- or LVX-treated mice.

Liver- and spleen-isolated neutrophils in all groups had a similar phenotype and activation status (based on CD11b expression) at 2 h after TNF administration. Thereafter, CD11b expression stabilized (Figs. 5A and B) in Veh+TNF- and LVX+TNF-treated mice, but in the TVX+TNF-treated mice the activation status of the liver- and spleen-derived neutrophils was increased (Figs. 5A and B).

Additionally, we checked blood for the presence and activation status of neutrophils. Interestingly, TVX+TNF treatment increased the number of neutrophils in blood at 2 h (Figure 6A), and these neutrophils displayed increased CD11b, and decreased CD62L and CD44 expression when compared with the other treatments (Figure 6A). In addition, flow cytometry of live blood $CD45.2^{+}/Ly6G^{+}$ cells without exclusion of aggregates showed an increased number of multicellular events (identified as LY6G+/FSC-W hi) in mice receiving TVX when compared with Veh- or LVX-treated mice (Figure 6B). This indicates the presence of homotypic and heterotypic neutrophil aggregates.

Effects of Ly6C+ Cell Depletion on Serum Levels and Hepatic Production of Cytokines

Using a neutrophil and monocyte depleting antibody (anti-Ly6C clone: RB6-8C5), we investigated whether the lack of these cells after TNF administration affected the inflammatory response, in particular with regard to LVX.

Two hours after the injection of the cytokine (TNF), depletion of neutrophils and monocytes resulted in a significant increase in the serum levels of MIP-2 when compared with the control (Figure 7A). In addition, depletion of neutrophils and monocytes increased the MIP-2 protein concentrations at 4 h in liver homogenates in Veh+PBS and LVX+TNF-treated mice (Figure 7B). Depletion did not affect hepatic MIP-2 concentration in mice receiving Veh+TNF and TVX+TNF (Figure 7B). Together data indicates that lack of Ly6C-positive cells results in increased chemotactic signals.

Depletion of neutrophils and monocytes also influenced IL-6 serum concentrations, and in particular elicited a ≈2-fold increase in IL-6 serum concentration in LVX+TNF and Veh+TNF-treated mice when compared with mice receiving the isotype antibody. Depletion did not change IL-6 levels resulting from TVX+TNF and Veh+PBS-treatments (Figure 7A). Notably, the IL-6 levels in depleted LVX+TNF and Veh+TNF-treated mice matched the concentrations observed in mice receiving TVX+TNF.

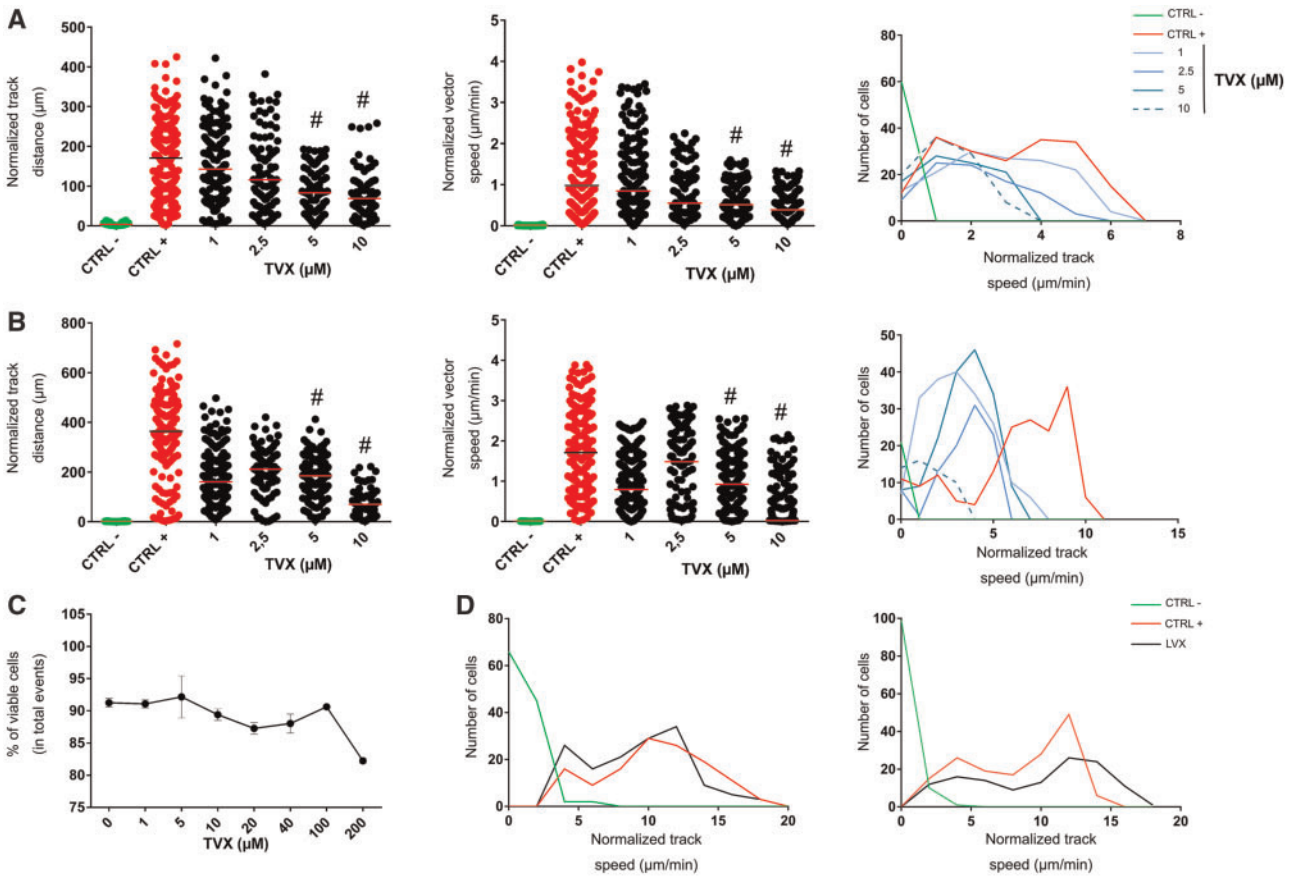

Figure 3. Impairment of human neutrophil chemotaxis toward sterile and nonsterile stimuli by TVX. Human neutrophils were obtained from healthy donors and immediately isolated and prepared for the 3D functional chemotaxis assay. The migration distance of neutrophils was normalized to the average migration path of neutrophils that were not stimulated with chemoattractants. A, B, Effects of increasing concentration of TVX were assessed on chemotaxis stimulated by f-MLF(A) and IL-8 (B). Dose-dependent effects on track distance, vector speed, and the distribution of track speeds are depicted. C, Neutrophil were tested for Annexin V and PI positivity 4 h after incubation with TVX. Percentage of double negative (Annexin V and PI) cells calculated in the total amount of analyzed events are presented. D, Effect of LVX (35 μM) on chemotaxis stimulated by f-MLF and IL-8. Distribution of track speeds are depicted. Presented data on chemotaxis are representative results for the experiments which were performed three times. # $p < .05$ when compared with cells treated with the positive control (CTRL+, A, f-MLF; B, IL-8), one-way ANOVA followed by Dunnett's post hoc test.

Serum concentrations of TNF in mice lacking neutrophils and monocytes were significantly higher than those observed in neutrophil/monocyte-competent TVX-treated mice 1 h after exogenous administration of the same cytokine. Both in TVX+TNF-treated and LVX+TNF-treated mice, depletion of Ly6C-positive cells resulted in an increase of serum levels of TNF when compared with the corresponding mice receiving the isotype antibody. This increase was 6-fold in LVX-treated mice and 2-fold in TVX-treated mice (Figure 7A).

Depletion of neutrophils and monocytes significantly decreased serum ALT concentration in TVX+TNF mice (Figure 7C), illustrating that these cells are partly responsible for the ultimate TVX-induced liver injury.

DISCUSSION

In our previous study, we have demonstrated that TVX delays the TNF-elicited influx of neutrophils and monocytes into the liver (Giustarini *et al.*, 2018). Here, we show that TVX blocks the PNX1 hemichannel in apoptotic hepatocytes during TVX+TNF-induced cell death. Additionally, we show that TVX inhibits the chemotactic movement of human neutrophils. Recently, others have shown that TVX is capable of blocking PNX1 which is involved in apoptosis (Poon *et al.*, 2014). In addition, it is known that PNX1 is crucial for optimal migration of leukocytes, neutrophils in particular (Bao *et al.*, 2013; Kukulski *et al.*, 2009). From our current new data, we conclude that blockade of the PNX1 by TVX represents an important event that has a dual effect related to the induction of DILI: it causes a decreased release of find-me signals and it hampers phagocyte migration toward attracting stimuli, increasing circulating TNF. The increased concentration of this cytokine, in the light of the capability of TVX to interact with TNF in inducing hepatocyte apoptosis (Beggs *et al.*, 2014; Shaw *et al.*, 2009d), represents a trigger for the development of liver injury.

The impairment in the PNX1-mediated release of molecules (find-me signals) during the mild TVX-induced apoptosis (Giustarini *et al.*, 2018) comprises a potentially toxic mechanism of TVX since the clearance of apoptotic cells relies on the release of find-me signals and the subsequent attraction of phagocytes (Chekeni *et al.*, 2010). Usually clearance of apoptotic cells is an immunologically silent process but if the apoptotic cells are not promptly removed they may undergo secondary necrosis leading to an uncontrolled released of inflammatory danger signals (Brauner *et al.*, 2013). Our conclusion that PNX1 blockade is involved in the delayed sequestration of phagocytes by TVX is also based on the knowledge that phagocytes follow

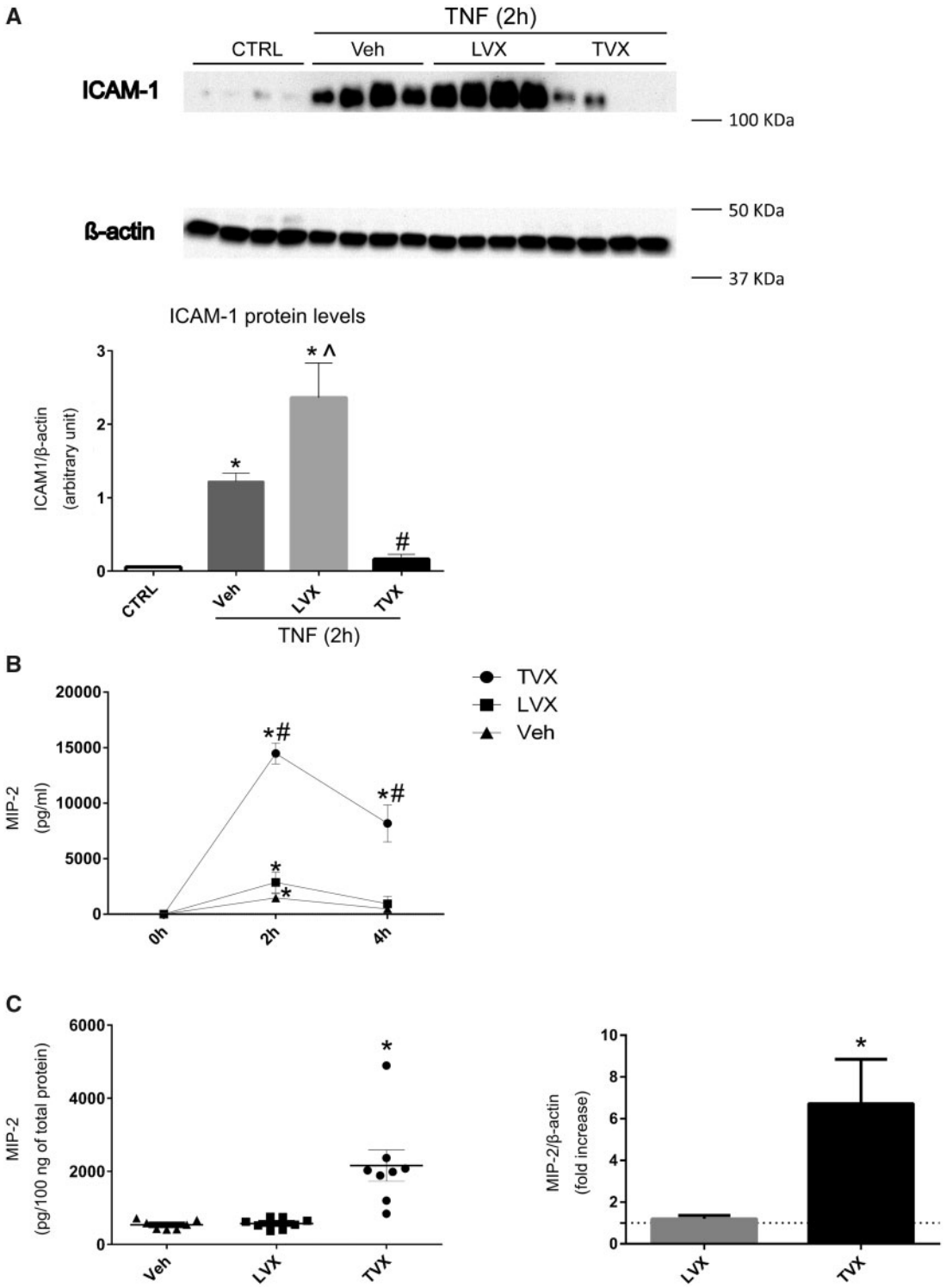

Figure 4. TVX reduced TNF-mediated ICAM-1 expression in the liver and increased serum and hepatic MIP-2 in mice. Mice (6 per treatment group) were treated with TVX, LVX or vehicle as depicted in Figure 1. Blood samples were collected at 0, 2, and 4 h after TNF injection. Liver lysates were obtained 2 h after TNF injection. Mice in control group (CTRL) only received the vehicle (no TNF). A, ICAM-1 protein levels in liver lysates. B, MIP-2 levels in serum. C, MIP-2 level in liver lysates. Liver tissue lysates obtained from mice sacrificed at 0 h were used to quantify MIP-2 mRNA by qPCR and protein by ELISA. Total amount of protein was determined by BCA protein assay kit. Data are presented as mean ± SEM. ● = TVX, ■ = LVX, ▲ = Veh; * $p < .05$ when compared with vehicle; # $p < .05$ when compared with LVX and TNF; ^ $p < .05$ when compared with Veh+TNF; one-way ANOVA followed by Dunnett's post hoc test.

chemotactic gradients (eg, of chemo-attractants such as f-MLF, IL-8) by means of PNX1-released ATP (Bao *et al.*, 2013; Chen *et al.*, 2010). As a result of the decreased motility of neutrophils in the sinusoids, recruitment will be delayed and the presence of these cells in the narrow vessels of the liver will be prolonged. Moreover, PNX1 blockade has also been shown to reduce

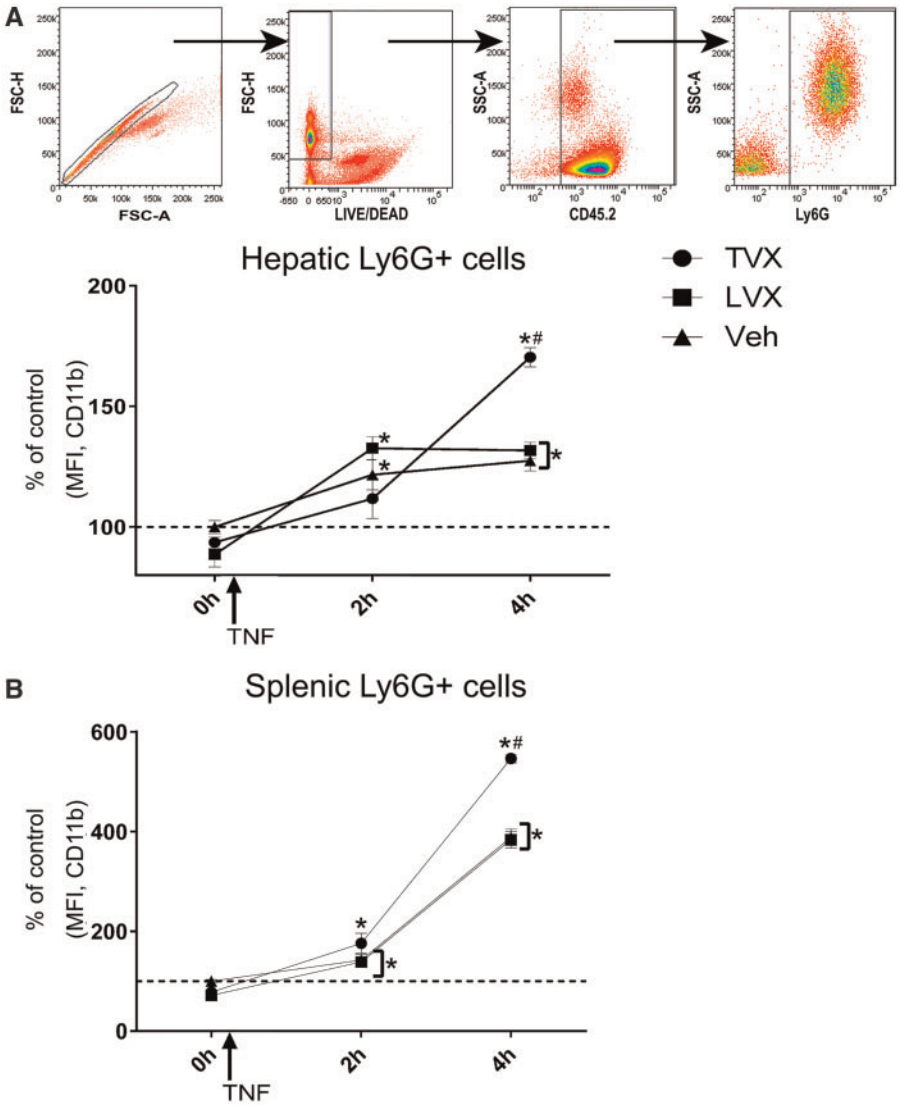

Figure 5. TVX induced intrahepatic neutrophil activation. Mice (8 per treatment group) were treated with TVX, LVX, or vehicle as depicted in Figure 1. Two hours after TNF injection, livers and spleens were processed to isolate leukocytes. A, Intrahepatic neutrophils were identified as CD45.2+/Ly6G+ live cells. Median fluorescent intensities (MFI) of CD11b on neutrophils are presented as percentage of the MFI observed in mice receiving only the Veh (no TNF, dashed line). B, Spleen neutrophils were identified as depicted in (A) and MFI presented as percentage of the MFI observed in mice receiving only the Veh (no TNF, dashed line). Data are presented as mean ± SEM.; ● = TVX, ■ = LVX, ▲ = Veh; * $p < .05$ when compared with vehicle; # $p < .05$ when compared to TNF; one-way ANOVA followed by Dunnett's post hoc test.

expression of adhesion molecules such as vascular cell adhesion molecule 1 (Lohman *et al.*, 2015), which is in agreement with our finding that TVX directly down-regulates expression of ICAM-1 in liver tissue, reducing the sequestration of leukocytes at the post-capillary venule level, where ICAM-1-dependent sequestration of leukocyte occurs (Kolaczkowska and Kubes, 2013).

In line with the importance of early recruitment of phagocytes in the protection of TVX-induced liver damage, depletion of Ly6C$^+$ cells elicited a greater systemic and hepatic early inflammatory response. Remarkably, depletion of Ly6C+ cells also caused increased inflammatory responses in TNF-only- and LVX+TNF-treated mice. These findings, together with previous works showing a synergistic effect of TVX with inflammatory stimuli (eg, TNF) causing hepatocyte apoptosis in vitro and in vivo (Beggs *et al.*, 2014; Shaw *et al.*, 2009a,d) confirms our conclusion that delay and lack in the recruitment of neutrophils and monocytes to the site of inflammation is at least partly responsible for the fluoroquinolone-induced hepatotoxicity (Giustarini *et al.*, 2018).

Our conclusion is in line with the consensus that neutrophils and monocytes not only initiate but also regulate inflammation (Soehnlein and Lindbom, 2010). In particular, depletion of neutrophils and monocytes has been associated with an increase in LPS- or infection-induced secretion of inflammatory cytokines such as TNF (Daley *et al.*, 2005, 2008; Hewett *et al.*, 1993; Holub *et al.*, 2009; Steinshamn and Bemelmans, 1995). However, the increase of inflammatory cytokines was insufficient to fully elicit LPS-induced liver injury (Hewett *et al.*, 1993), suggesting that neutrophils are still central for the onset of the damage. Although these findings clearly point to a pivotal role for neutrophils and monocytes in the regulation of early TNF-mediated inflammation, we did not formally rule out that depleting antibody administration may have effects which can

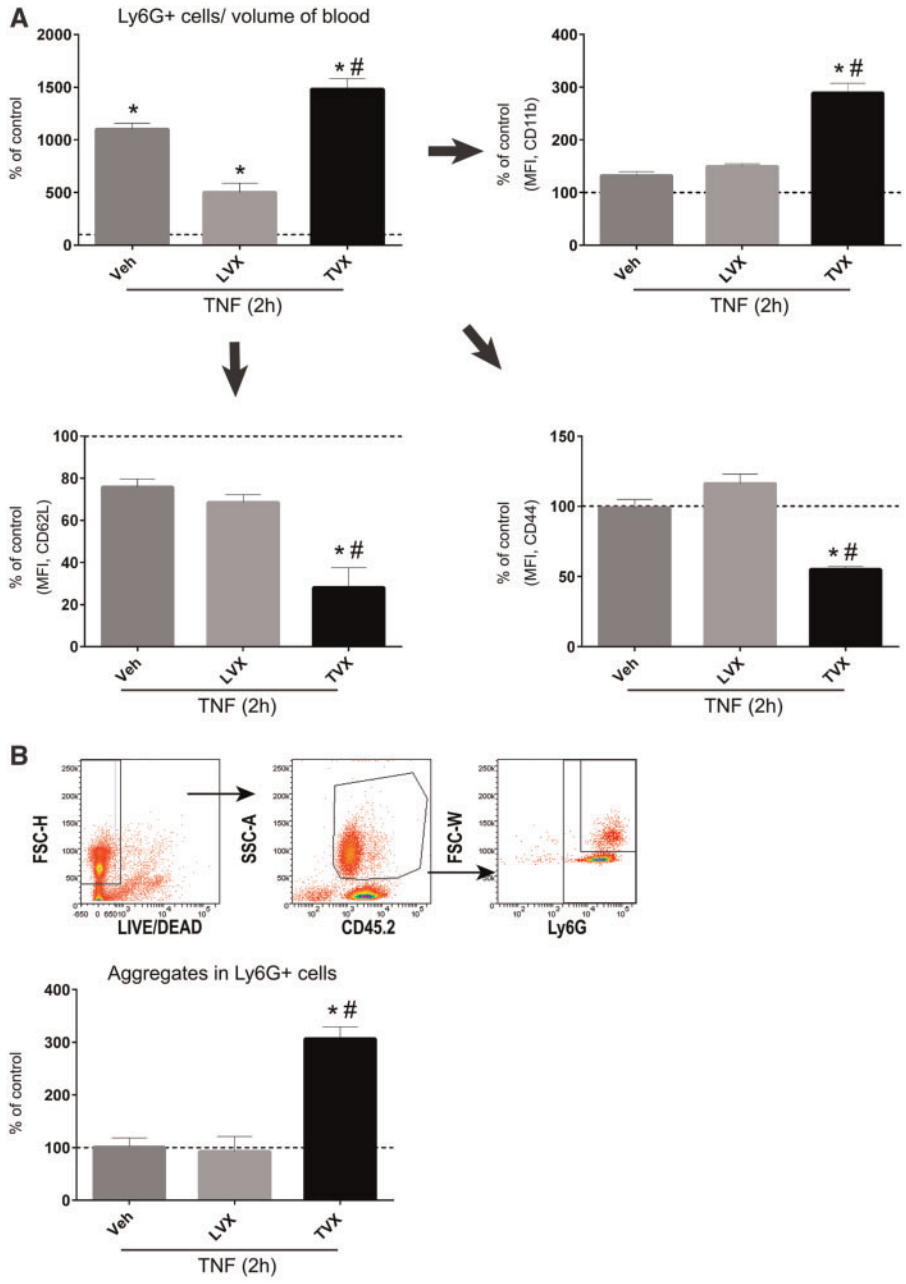

Figure 6. TVX-induced early activation of neutrophils in blood. Mice (8 per treatment group) were treated with TVX, LVX, or vehicle as depicted in Figure 1. Two hours after TNF injection, livers and spleens obtained from mice at each time point indicated were processed to isolate leukocytes. Blood was collected from inferior vena cava in heparin-coated tubes. Cells were counted and prepared for flow cytometry. A, Neutrophils were identified as CD45.2+/Ly6G+ live cells. Median fluorescent intensities (MFI) of CD11b, CD62L, and CD44 on neutrophils are presented as percentage of the MFI observed in mice receiving only the Veh (no TNF, dashed line). B, Ly6G+ aggregates were analyzed by inclusion of doublets, and presented as percentage of mice only receiving the Veh (no TNF, dashed line). Data are presented as mean ± SEM; ● = TVX, ■ = LVX, ▲ = Veh; * $p < .05$ when compared with vehicle; # $p < .05$ when compared with TNF; one-way ANOVA followed by Dunnett's post hoc test.

contribute to the observed cytokine increase. On the other hand, we can rule out the possibility that the increased cytokine levels may be due to apoptotic neutrophils induced by depleting antibody administration. Indeed, as demonstrated by Ren and colleagues, apoptotic neutrophils exert rather an anti-inflammatory effect on LPS-induced inflammation (Ren *et al.*, 2008). In line with this, others (Yu *et al.*, 2007) showed that depletion of neutrophils and monocytes is associated with a protective early gene response to dying neutrophils into the liver rather than with an increased susceptibility to inflammatory cytokine release. This is in line with findings from Shaw *et al.* (2009b) and our present results on TVX. On the contrary, the hepatic neutrophilia that we observed in mice treated with LVX+TNF did not lead to liver injury (Giustarini *et al.*, 2018), indicating that mere recruitment of neutrophils due to TNF injection is also not sufficient to elicit DILI. We therefore propose that in case of LVX+TNF- or Veh+TNF- treated mice neutrophils are sequestered in organs (such as liver) to regulate inflammation. In contrast, in TVX-treated mice, delayed neutrophils do not inhibit inflammation in the liver,

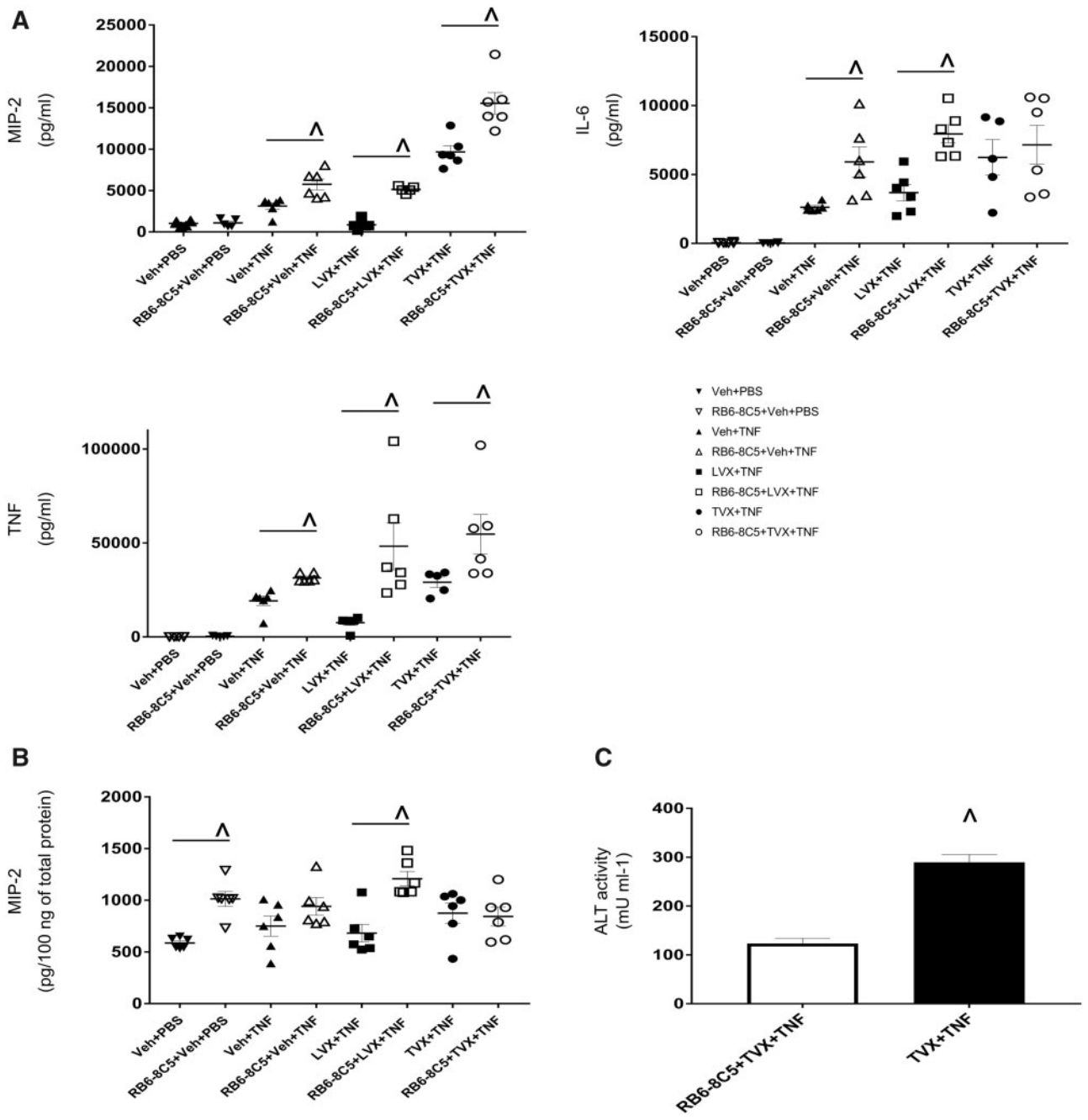

Figure 7. Lack of monocytes and neutrophils led to increased serum and hepatic inflammatory cytokines. Mice were administered with anti-Ly6C (clone: RB6-8C5) or its correspondent isotype (IgG2b) 72 and 24 h before receiving the drug solutions. A, Serum cytokines (MIP-2, IL-6, and TNF) were assessed on serums collected 2 h after TNF injection. B, Hepatic MIP-2 concentration was assessed on liver homogenates obtained from livers excised 4 h after TNF injection. Total amount of protein was determined by BCA protein assay kit. C, Serum ALT levels of depleted (RB6-8C5) and competent TVX+TNF-treated mice were assessed on samples collected 4 h after the injection of TNF. ALT levels were determined by colorimetric assay for ALT activity. Data are presented as mean ± SEM; ● = TVX +TNF; ○ = RB6-8C5+TVX+TNF, ■ = LVX+TNF, □ = RB6-8C5+LVX+TNF, ▲ = Veh+TNF, △ = RB6-8C5+Veh+TNF, ▼ = Veh+PBS, ▽ = RB6-8C5+Veh+PBS; ^ $p < .05$ when compared with neutrophil and monocyte depleted mice receiving the same drug treatment or the correspondent vehicle; one-way ANOVA followed by Dunnett's post hoc test.

become activated, form aggregates that accumulate in the liver vessels.

Importantly with regard to TVX-induced DILI, initial TVX effects (mild apoptosis, disrupted release of find-me signals, hampered tissue influx, and aggregate formation of phagocytes) appear to be linked to the intravascular activation of neutrophils (Neelamegham *et al.*, 2000; Simon *et al.*, 1993). Thus, neutrophil aggregates are impeded in their capability to pass the narrow sinusoids and once intravascularly activated (Borregaard *et al.*, 1994; Sheshachalam *et al.*, 2014), they eventually will cause vascular damage and allow late influx of inflammatory leukocytes into the tissue causing DILI, as also shown by Shaw *et al.* (2009b,c). The observed impairment of sequestration of leukocytes in the liver of TVX-treated mice may also support previous findings showing an impaired clearance of TNF in mice treated with TVX (Shaw *et al.*, 2009a). Possibly, when due

to TVX neutrophils and monocytes cannot provide their anti-phlogistic action in the liver, resident macrophages keep on producing TNF (but also other pro-inflammatory cytokines) which, in addition, is not properly eliminated by neutrophil-derived soluble TNF receptors (sTNFR) (Jablonska *et al.*, 1999; Lantz *et al.*, 1994; Shaw *et al.*, 2009a; Steinshamn and Bemelmans, 1995). Indeed, the release of sTNFR by neutrophils and monocytes occurs especially when these cells adhere to surfaces via both integrin and non-integrin-dependent mechanisms (Lantz *et al.*, 1994).

It is also known that activated neutrophils release proteolytic enzymes such as elastase. Elastase has been demonstrated to be crucial in final TVX-induced liver damage (Shaw *et al.*, 2009c) and in the reduction of the IL-8 receptor on the neutrophil surface (Bakele *et al.*, 2014). Also in our experiments, neutrophil activation represents a crucial step in the sequence of events leading to TVX-induced liver damage as confirmed by the reduced serum ALT concentration at 4 h in mice depleted of neutrophils. The intravascular activation of neutrophils as fundamental step in the damage mediated by TVX is also in line with the increased amount of plasminogen activator inhibitor-1 (PAI-1) in mice receiving TVX+LPS (Shaw *et al.*, 2009b), and with the beneficial effects of heparin administration on TVX+LPS-induced DILI. Of note, the decrease of ICAM-1 may be reinforced by increased degranulation of activated neutrophils (Champagne *et al.*, 1998).

Recent observations on the incidence of DILI by antibiotic use emphasize the urgency to clarify the mechanisms underlying fluoroquinolone-induced DILI (Chalasani *et al.*, 2015). In addition, previous studies suggest that the development of TVX-induced liver injury is related to multiple effects of TVX+TNF combination (neutrophils, pro-inflammatory cytokines, and alterations of hemostasis) which seem to represent segregated mechanistic pathways (Shaw *et al.*, 2009b). Interestingly, the mechanism of TVX-induced liver injury involving dysregulation of innate immune responses as proposed here is consistent with the rapid onset of DILI associated with fluoroquinolones in patients (Orman *et al.*, 2011) and explains the liaison between the apparently segregated toxic pathways identified previously by Shaw *et al.*(2009b). Moreover, other pharmaceuticals (such as diclofenac, chlorpromazine, amiodarone and ranitidine) have been associated with the induction of liver injury and hepatocyte apoptosis when combined with inflammatory mediators in vivo and in vitro, respectively (Deng *et al.*, 2006; Gandhi *et al.*, 2013; Lu *et al.*, 2012; Luyendyk *et al.*, 2003). In our opinion, this indicates the urge to investigate if other DILI-associated compounds dysregulate early recruitment of phagocytes during inflammation.

With regard to risks of DILI by fluoroquinolones, impairment of innate immune responses in elderly patients (Brubaker *et al.*, 2011) may represent an idiosyncratic factor explaining the higher incidence of fluoroquinolone-induced events in this population (Hayashi and Chalasani, 2012). Our data provides novel insights on leukocyte-mediated regulation of early inflammation and its role in the onset of DILI.

FUNDING

This work was supported by the European Community (Grant number MIP-DILI-115336). The Mechanism-Based Integrated Systems for the Prediction of Drug-Induced Liver Injury (MIP-DILI) project has received support from the Innovative Medicines Initiative Joint Undertaking, resources of which are composed of financial contribution from the European Union's Seventh Framework Programme (FP7/20072013) and EFPIA companies' in-kind contribution. http://www.imi.europa.eu/.

REFERENCES

Bakele, M., Lotz-Havla, A. S., Jakowetz, A., Carevic, M., Marcos, V., Muntau, A. C., Gersting, S. W., and Hart, D. (2014). An interactive network of elastase, secretases, and PAR-2 protein regulates CXCR1 receptor surface expression on neutrophils. *J. Biol. Chem.* **289**, 20516–20525.

Bao, Y., Chen, Y., Ledderose, C., Li, L., and Junger, W. G. (2013). Pannexin 1 channels link chemoattractant receptor signaling to local excitation and global inhibition responses at the front and back of polarized neutrophils. *J. Biol. Chem.* **288**, 22650–22657.

Beggs, K. M., Fullerton, A. M., Miyakawa, K., Ganey, P. E., and Roth, R. A. (2014). Molecular mechanisms of hepatocellular apoptosis induced by trovafloxacin-tumor necrosis factor-alpha interaction. *Toxicol Sci.* **137**, 91–101.

Borregaard, N., Kjeldsen, L., Sengeløv, H., Diamond, M. S., Springer, T. A., Anderson, H. C., Kishimoto, T. K., and Bainton, D. F. (1994). Changes in subcellular localization and surface expression of L-selectin, alkaline phosphatase, and Mac-1 in human neutrophils during stimulation with inflammatory mediators. *J. Leukoc. Biol.* **56**, 80–87.

Brauner, J. M., Schett, G., Herrmann, M., and Muñoz, L. E. (2013). No littering: The clearance of dead cells and leaking cellular contents and possible pathological complications. *OA Arthritis* **1**, 1–7.

Brubaker, A. L., Palmer, J. L., and Kovacs, E. J. (2011). Age-related dysregulation of inflammation and innate immunity: Lessons learned from rodent models. *Aging Dis.* **2**, 346–360.

Chalasani, N., Bonkovsky, H. L., Fontana, R., Lee, W., Stolz, A., Talwalkar, J., Reddy, K. R., Watkins, P. B., Navarro, V., Barnhart, H., *et al.* (2015). Features and outcomes of 899 patients with drug-induced liver injury: The DILIN prospective study. *Gastroenterology* **148**, 1340–1352.e7.

Champagne, B., Tremblay, P., Cantin, A., and St. Pierre, Y. (1998). Proteolytic cleavage of ICAM-1 by human neutrophil elastase 1. *J. Immunol.* **161**, 6398–6405.

Chekeni, F. B., Elliott, M. R., Sandilos, J. K., Walk, S. F., Kinchen, J. M., Lazarowski, E. R., Armstrong, A. J., Penuela, S., Laird, D. W., Salvesen, G. S., *et al.* (2010). Pannexin 1 channels mediate "find-me" signal release and membrane permeability during apoptosis. *Nature* **467**, 863–867.

Chen, Y., Yao, Y., Sumi, Y., Li, A., To, U. K., Elkhal, A., Inoue, Y., Woehrle, T., Zhang, Q., Hauser, C., *et al.* (2010). Purinergic signaling: A fundamental mechanism in neutrophil activation. *Sci. Signal.* **3**, ra45.

Crispe, I. N. (2001). Isolation of mouse intrahepatic lymphocytes. *Curr. Protoc. Immunol.* Chapter **3**, Unit 3.21.

Daley, J. M., Ivanenko-Johnston, T., Reichner, J. S., and Albina, J. E. (2005). Transcriptional regulation of TNF-alpha production in neutropenia. *Am. J. Physiol. Regul. Integr. Comp. Physiol.* **288**, R409–R412.

Daley, J. M., Thomay, A. A., Connolly, M. D., Reichner, J. S., and Albina, J. E. (2008). Use of Ly6G-specific monoclonal antibody to deplete neutrophils in mice. *J. Leukoc. Biol.* **83**, 64–70.

Deng, X., Stachlewitz, R. F., Liguori, M. J., Blomme, E. a G., Waring, J. F., Luyendyk, J. P., Maddox, J. F., Ganey, P. E., and Roth, R. A. (2006). Modest inflammation enhances diclofenac

hepatotoxicity in rats: Role of neutrophils and bacterial translocation. *J. Pharmacol. Exp. Ther.* **319**, 1191–1199.

Gandhi, A., Guo, T., Shah, P., Moorthy, B., and Ghose, R. (2013). Chlorpromazine-induced hepatotoxicity during inflammation is mediated by TIRAP-dependent signaling pathway in mice. *Toxicol. Appl. Pharmacol.* **266**, 430–438.

Giustarini, G., Kruijssen, L., Roest, M. V., Bleumink, R., Weaver, R. J., Bol, M., Joost, S., and Raymond, S. (2018). Tissue influx of neutrophils and monocytes is delayed during development of trovafloxacin-induced tumor necrosis factor-dependent liver injury in mice. *J. Appl. Toxicol.* **38**, 753–765.

Hayashi, P. H., and Chalasani, N. P. (2012). Liver injury in the elderly due to fluoroquinolones: Should these drugs be avoided? *Cmaj* **184**, 1555–1556.

Hewett, J. A., Jean, P. A., Kunkel, S. L., and Roth, R. A. (1993). Relationship between tumor necrosis factor-alpha and neutrophils in endotoxin-induced liver injury. *Am. J. Physiol.* **265**, G1011–G1015.

Holub, M., Cheng, C.-W., Mott, S., Wintermeyer, P., van Rooijen, N., and Gregory, S. H. (2009). Neutrophils sequestered in the liver suppress the proinflammatory response of Kupffer cells to systemic bacterial infection. *J. Immunol.* **183**, 3309–3316.

Jablonska, E., Jablonski, J., and Holownia, A. (1999). Role of neutrophils in release of some cytokines and their soluble receptors. *Immunol. Lett.* **70**, 191–197.

Kolaczkowska, E., and Kubes, P. (2013). Neutrophil recruitment and function in health and inflammation. *Nat. Rev. Immunol.* **13**, 159–175.

Kukulski, F., Ben Yebdri, F., Lecka, J., Kauffenstein, G., Lévesque, S. A., Martín-Satué, M., and Sévigny, J. (2009). Extracellular ATP and P2 receptors are required for IL-8 to induce neutrophil migration. *Cytokine* **46**, 166–170.

Lantz, M., Björnberg, F., Olsson, I., and Richter, J. (1994). Adherence of neutrophils induces release of soluble tumor necrosis factor receptor forms. *J. Immunol.* **152**, 1362–1369.

Lohman, A. W., Leskov, I. L., Butcher, J. T., Johnstone, S. R., Stokes, T. A., Begandt, D., DeLalio, L. J., Best, A. K., Penuela, S., Leitinger, N., *et al.* (2015). Pannexin 1 channels regulate leukocyte emigration through the venous endothelium during acute inflammation. *Nat. Commun.* **6**, 7965.

Lu, J., Jones, A. D., Harkema, J. R., Roth, R. A., and Ganey, P. E. (2012). Amiodarone exposure during modest inflammation induces idiosyncrasy-like liver injury in rats: Role of tumor necrosis factor-alpha. *Toxicol. Sci.* **125**, 126–133.

Lu, J., Miyakawa, K., Roth, R. A., and Ganey, P. E. (2013). Tumor necrosis factor-alpha potentiates the cytotoxicity of amiodarone in Hepa1c1c7 cells: Roles of caspase activation and oxidative stress. *Toxicol. Sci.* **131**, 164–178.

Luyendyk, J. P., Maddox, J. F., Cosma, G. N., Ganey, P. E., Cockerell, G. L., and Roth, R. A. (2003). Ranitidine treatment during a modest inflammatory response precipitates idiosyncrasy-like liver injury in rats. *J. Pharmacol. Exp. Ther.* **307**, 9–16.

Matzer, S. P., Baumann, T., Lukacs, N. W., Röllinghoff, M., and Beuscher, H. U. (2001). Constitutive expression of macrophage-inflammatory protein 2 (MIP-2) mRNA in bone marrow gives rise to peripheral neutrophils with preformed MIP-2 protein. *J. Immunol.* **167**, 4635–4643.

Neelamegham, S., Taylor, A. D., Shankaran, H., Smith, C. W., and Simon, S. I. (2000). Shear and time-dependent changes in Mac-1, LFA-1, and ICAM-3 binding regulate neutrophil homotypic adhesion. *J. Immunol.* **164**, 3798–3805.

Orman, E. S., Conjeevaram, H. S., Vuppalanchi, R., Freston, J. W., Rochon, J., Kleiner, D. E., and Hayashi, P. H. (2011). Clinical and histopathologic features of fluoroquinolone-induced liver injury. *Clin. Gastroenterol. Hepatol.* **9**, 517–523.e3.

Overbeek, S. A., Braber, S., Koelink, P. J., Henricks, P. A. J., Mortaz, E., LoTam Loi, A. T., Jackson, P. L., Garssen, J., Wagenaar, G. T. M., and Timens, W. (2013). Cigarette smoke-induced collagen destruction; key to chronic neutrophilic airway inflammation? *PLoS One* **8**, e55612.

Poon, I. K. H., Chiu, Y.-H., Armstrong, A. J., Kinchen, J. M., Juncadella, I. J., Bayliss, D. A., and Ravichandran, K. S. (2014). Unexpected link between an antibiotic, pannexin channels and apoptosis. *Nature* **507**, 329–334.

Ren, Y., Xie, Y, Jiang, G., Fan, J., Yeung, J., Li, W., Tam, P. K. H., and Savill, J. (2008). Apoptotic cells protect mice against lipopolysaccharide-induced shock. *J Immunol.* **180**, 4978–85.

Shaw, P. J., Beggs, K. M., Sparkenbaugh, E. M., Dugan, C. M., Ganey, P. E., and Roth, R. A. (2009a). Trovafloxacin enhances TNF-induced inflammatory stress and cell death signaling and reduces TNF clearance in a murine model of idiosyncratic hepatotoxicity. *Toxicol. Sci.* **111**, 288–301.

Shaw, P. J., Fullerton, A. M., Scott, M. A., Ganey, P. E., and Roth, R. A. (2009b). The role of the hemostatic system in murine liver injury induced by coexposure to lipopolysaccharide and trovafloxacin, a drug with idiosyncratic liability. *Toxicol. Appl. Pharmacol.* **236**, 293–300.

Shaw, P. J., Ganey, P. E., and Roth, R. A. (2009c). Trovafloxacin enhances the inflammatory response to a gram-negative or a gram-positive bacterial stimulus, resulting in neutrophil-dependent liver injury in mice. *J. Pharmacol. Exp. Ther.* **330**, 72–78.

Shaw, P. J., Ganey, P. E., and Roth, R. A. (2009d). Tumor necrosis factor α is a proximal mediator of synergistic hepatotoxicity from trovafloxacin/lipopolysaccharide coexposure. *J. Pharmacol. Exp. Ther.* **328**, 62–68.

Shaw, P. J., Hopfensperger, M. J., Ganey, P. E., and Roth, R. A. (2007). Lipopolysaccharide and trovafloxacin coexposure in mice causes idiosyncrasy-like liver injury dependent on tumor necrosis factor-alpha. *Toxicol. Sci.* **100**, 259–266.

Sheshachalam, A., Srivastava, N., Mitchell, T., Lacy, P., and Eitzen, G. (2014). Granule protein processing and regulated secretion in neutrophils. *Front. Immunol.* **5**, 1–11.

Simon, S. I., Rochon, Y. P., Lynam, E. B., Smith, C. W., Anderson, D. C., and Sklar, L. A. (1993). Beta 2-integrin and L-selectin are obligatory receptors in neutrophil aggregation. *Blood* **82**, 1097–1106.

Soehnlein, O., and Lindbom, L. (2010). Phagocyte partnership during the onset and resolution of inflammation. *Nat. Rev. Immunol.* **10**, 427–439.

Steinshamn, S., and Bemelmans, M. (1995). Granulocytopenia reduces release of soluble TNF receptor p75 in endotoxin-stimulated mice: A possible mechanism of enhanced TNF activity. *Cytokine* **7**, 50–6.

Vincent, J., Teng, R., Dalvie, D. K., and Friedman, H. L. (1998). Pharmacokinetics and metabolism of single oral doses of trovafloxacin. *Am. J. Surg.* **176**, 8S–13S.

Yu, M-L., Dai, C-Y., and Chuang, W-L. (2007). Neutrophil Depletion Protects Against Murine Acetaminophen Hepatotoxicity: Another Perspective. *Hepatology* **45**, 1587–1588.